



Deposited via The University of Sheffield.

White Rose Research Online URL for this paper:

<https://eprints.whiterose.ac.uk/id/eprint/142324/>

Version: Accepted Version

---

**Proceedings Paper:**

Quan, G., Huang, S.S. and Burgess, I. (2017) 10.10: Influence of beam-end buckling on adjacent beam-column connections in fire. In: Ce/Papers. Eurosteel 2017, 13-15 Sep 2017, Copenhagen, Denmark. Ernst & Sohn Verlag, pp. 2592-2600. ISSN: 2509-7075.

<https://doi.org/10.1002/cepa.308>

---

This is the accepted version of the following article: Quan, G. , Huang, S. and Burgess, I. (2017), 10.10: Influence of beam-end buckling on adjacent beam-column connections in fire. ce/papers, 1: 2592-2600, which has been published in final form at <https://doi.org/10.1002/cepa.308>. This article may be used for non-commercial purposes in accordance with the Wiley SelfArchiving Policy.

**Reuse**

Items deposited in White Rose Research Online are protected by copyright, with all rights reserved unless indicated otherwise. They may be downloaded and/or printed for private study, or other acts as permitted by national copyright laws. The publisher or other rights holders may allow further reproduction and re-use of the full text version. This is indicated by the licence information on the White Rose Research Online record for the item.

**Takedown**

If you consider content in White Rose Research Online to be in breach of UK law, please notify us by emailing [eprints@whiterose.ac.uk](mailto:eprints@whiterose.ac.uk) including the URL of the record and the reason for the withdrawal request.

# Influence of Beam-End Buckling on Adjacent Beam-Column Connections in Fire

Guan Quan\*, Shan-Shan Huang, Ian Burgess

University of Sheffield, Dept. Civil and Structural Engineering, UK

quanguan1212@gmail.com

s.huang@sheffield.ac.uk

ian.burgess@sheffield.ac.uk

## ABSTRACT

An analytical model to simulate the beam-end buckling phenomenon, which occurs particularly in the fire context, has been developed. In this research, a component-based beam-end buckling element has for the first time been created for beams of Classes 1 and 2. The component-based buckling element is composed of nonlinear springs, which can deal with loading-unloading-reloading paths. A significant challenge is to enable the flange-buckling component to deal with a descending post-buckling path simultaneously with deformation-reversal, because more than one solution can be found at a single force level in the solution process. The buckling element has been implemented in the structural fire engineering software *Vulcan*, so that it can be used adjacent to existing connection elements in frame modelling. The effects of the buckling element have been investigated in frame analysis using *Vulcan*. It has been shown that, in most cases, the stresses within the connection's bolt rows tend to decrease when the buckling element is taken into consideration. By ignoring the buckling element near to the beam-to-column connections in structural fire analysis, the results tend to be on the safe side regarding the connection forces.

**Keywords:** Beam-end buckling, Post-buckling, Component-based model, Connections, Fire

## 1 INTRODUCTION

The investigation of the “7 World Trade” collapse in New York City [1] indicated that the building collapse was triggered by the failure of beam-to-column joints as a result of restraint to large thermal expansions of beams. This illustrated that joints are among the most vulnerable elements of buildings in fire. Joint fracture may initiate the collapse of a single beam, which may trigger a sequence of further connection failures, possibly leading to progressive collapse of a whole building. It is important to investigate the phenomena involved in restrained expansion of beams, especially those which can influence the force distributions of connection bolt rows.

The combination of beam-web shear buckling and beam bottom-flange buckling, near to the ends of steel beams, was commonly seen in the full-scale Cardington Fire Tests [2], as shown in Fig. 1. This phenomenon can clearly affect the bolt-row force distributions of the adjacent connections, as well as the behaviour of the beam itself, at high temperatures. Previous researchers [3-5] have investigated the behaviour of various types of joint at high temperature. However, buckling in the beam-ends in the vicinity of connections has not previously been sufficiently investigated, and cannot be simulated in high-temperature global frame analysis. The changes in the distribution of forces within beam-to-column connections caused by beam-end buckling could potentially cause earlier fractures and lead to the possibility of progressive collapse being ignored in structural fire engineering design.

In this research, the influences of the beam-end buckling phenomena on the adjacent connections, as well as on the wider beam/frame interaction behaviour, have been investigated. The objective of this paper is to discuss the effects of local beam-end buckling on connection forces, and to suggest how the results from global modelling can be considered when the buckling phenomena are ignored in practical design.

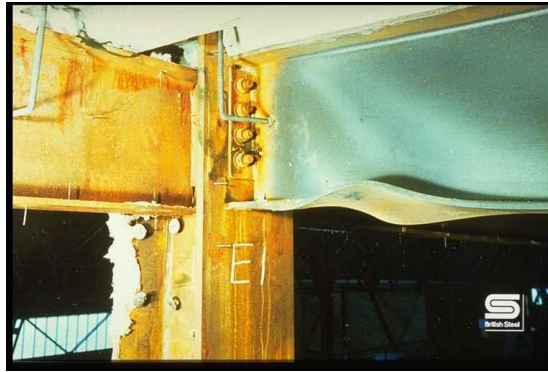


Fig. 1. Flange buckling and beam-web shear buckling in combination [6]

## 2 CREATION OF THE COMPONENT-BASED MODEL

### 2.1 Overall components of the component-based model

The proposed yield line mechanism of the beam-end buckling phenomena, including beam-web shear buckling and bottom-flange buckling in the analytical model, is shown in Fig. 2(a). The derivation of equilibrium equations for the analytical model is based on equality of the internal work in the buckling zone and the loss of potential of the externally applied load. The buckling zone can be represented by a component-based model. This model is shown in Fig. 2(b) as the *Buckling Element*. In Fig. 2(b), the component-based *Connection Element* adjacent to the buckling element is typical of those representing a component-based flush end-plate connection. According to the analytical model introduced by the authors [7], the component-based buckling element can be divided into top-flange springs, bottom-flange springs and a web shear spring. To represent the flange actions, pairs of springs, one to act only in tension and the other to act only in compression, are located at each flange, representing its resistance. For the pair of springs at either location, only one spring will be activated at any instant, depending on the sense of the spring force.

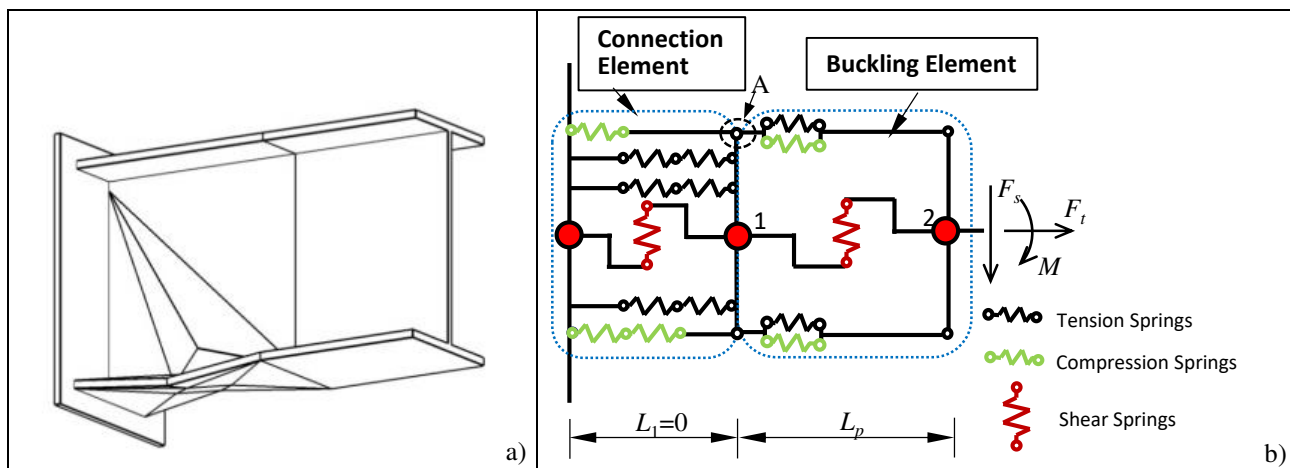


Fig. 2. Beam-end buckling model: a) Yield line mechanism; b) Component-based model

According to the existing analytical model [7], the characteristics of the flange springs and the shear spring can be represented in the form shown in Fig. 23.

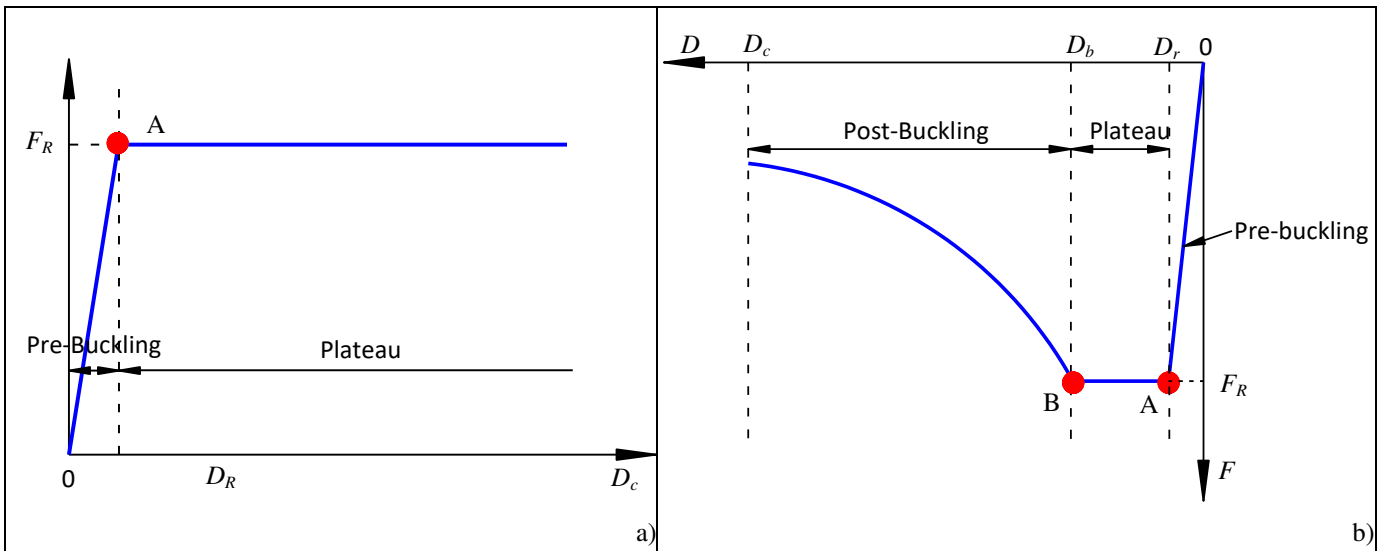


Fig. 3. Spring characteristics at a constant temperature: a) Tension spring; b) Compression and shear springs

## 2.2 Deformation reversal of springs at a constant temperature

During the course of a fire, the beam-end buckling element can experience complex changes of horizontal force and movement caused by material and geometric nonlinearity, as well as by restraint to thermal expansion. These forces will be equilibrated by the horizontal springs at the flanges, which can be subject to either compression or tension at different stages of loading/heating. The flange springs were created to be able to deal with loading-unloading-reloading paths at varying temperatures during the course of a fire. The vertical shear spring does not need a reversal path, as reversal of shear would require very unusual circumstances. The loading-unloading-reloading path is governed by a modified Masing Rule [8]. In the Masing Rule, the component characteristics of a spring can be represented by the combination of a “skeleton” curve and a “hysteresis” curve. A schematic illustration of the Masing Rule is shown in Fig. 4(a). The hysteresis curve is the skeleton curve scaled by a factor of two and rotated by 180°. The force-deflection relationship is initially on the skeleton curve until displacement reversal occurs at Point A, after which the force-displacement relationship follows the hysteresis curve. For the springs in the component-based model, the linear part of the unloading curve finishes exactly at the point where it meets the horizontal axis; this intersection is defined as the “Reference Point”, and represents the permanent deformation which has been accumulated. The point at which deformation reversal initiates is defined as the “Intersection Point”.

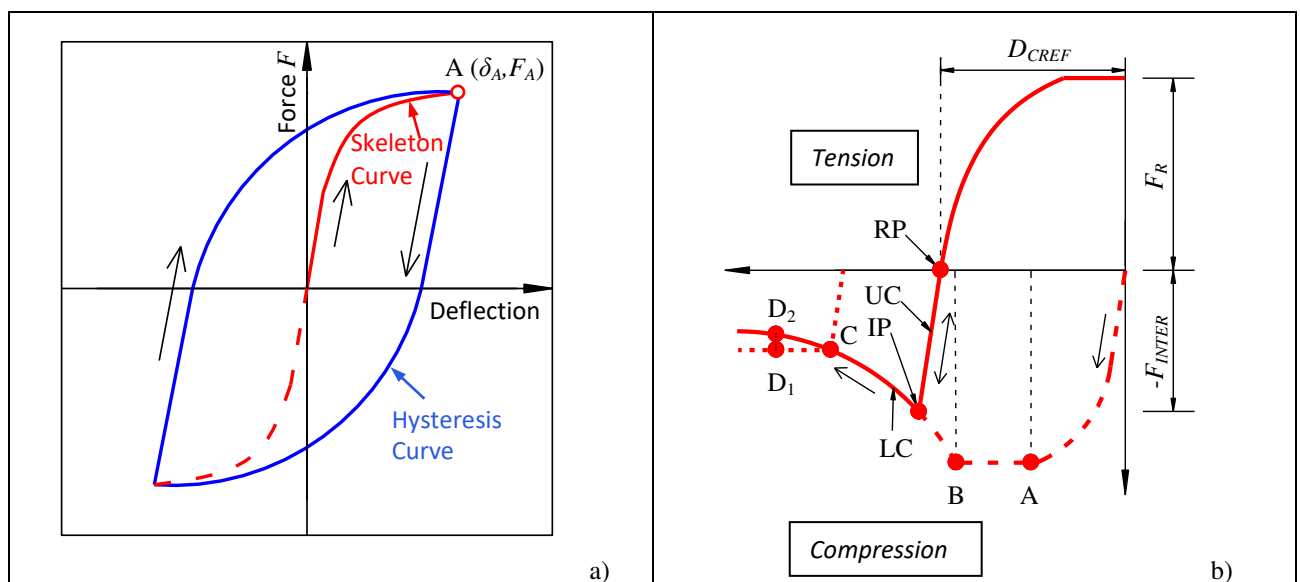


Fig. 4. Deformation reversal: a) A schematic illustration of application of the Masing Rule; b) An example in the post-buckling stage

Fig. 4(b) illustrates the situation when deformation reversal occurs in the post-buckling stage. A significant challenge is to enable the flange-buckling component to deal with a descending post-buckling path simultaneously with deformation-reversal, because more than one solution can be found at a single force level in the solution process. In order to solve this problem, taking as an example the situation when the deformation reversal initiates at Point C in Fig. 4 (b), for the loading path, a ‘zero’ stiffness (instead of a negative stiffness) is assumed to define the start of the next iteration. The unloading path remains unchanged. The loading and unloading paths become the dashed lines starting from Point C. When the internal force is larger than the external, the iteration will follow the unloading path. Otherwise, the loading path is adopted, in which case Point D<sub>1</sub> is assumed to be the end of this iteration. It is assumed that the initiation point of the next iteration is Point D<sub>2</sub>, which has the same deformation as D<sub>1</sub> but is on the real post-buckling curve.

### 2.3 Deformation reversal of springs at elevated temperatures

At elevated temperatures, different characteristic stress-strain curves are defined for different temperatures. The essential assumption for displacement-reversal as temperatures increase is that the Reference Point of the unloading curve does not change between two successive temperature steps. The new unloading path will still be linear, following the initial slope of the force-deformation relationship at the new temperature, and so the Intersection Point (at which unloading initiates) is relocated. Taking the compression spring in the “plateau” stage as an example, Fig. 5 shows the loading and unloading procedure when the spring’s temperature increases.

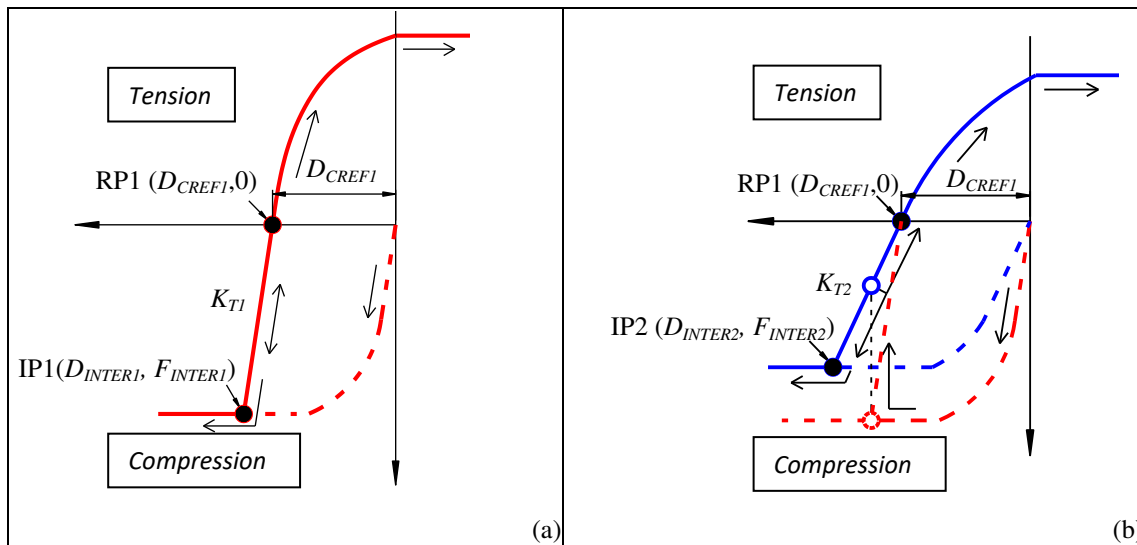


Fig. 5. Loading and unloading procedure when temperature increases: (a) At temperature  $T_1$ ; (b) At temperature  $T_2$  ( $T_2 > T_1$ )

At temperature  $T_1$ , the deformation at the Reference Point can be calculated using

$$D_{CREF1} = D_{INTER1} - F_{INTER1} / K_{T1} \quad (1)$$

where  $D_{CREF1}$  is the position of the Reference Point at temperature  $T_1$ ,  
 $D_{INTER1}$  is the spring deformation at which deformation reversal initiates,  
 $F_{INTER1}$  is the spring force at which deformation reversal initiates,  
 $K_{T1}$  is the spring Young’s Modulus at temperature  $T_1$ .

When the temperature increases to  $T_2$ , the Reference Point remains identical, while a new position of the Intersection Point at  $T_2$  can be found using the new initial elastic stiffness  $K_{T_2}$ . The spring deformation of the new Intersection Point is,

$$D_{INTER2} = D_{CREF1} + F_{R2} / K_{T2} \quad (2)$$

where  $D_{INTER2}$  is the new position of the Intersection Point at temperature  $T_2$ ,

$F_{R2}$  is the spring yield force at temperature  $T_2$ ,

$K_{T2}$  is the Young's Modulus at temperature  $T_2$ .

It is assumed that the deformation of the spring remains identical during the change between adjacent temperature transition steps. Therefore, the real spring position falls to the unloading curve at temperature  $T_2$  from the Intersection Point, for which deformation reversal initiates at temperature  $T_1$ . This jump disturbs the force equilibrium, and the spring needs to find a new deformation to establish the force equilibrium at  $T_2$ .

### 3 FRAME ANALYSIS

In order to demonstrate the possibility of carrying out performance-based global analysis which includes the buckling element in *Vulcan*, and to conduct a preliminary study the influence of the buckling element on its adjacent connection, a two-storey two-span plane frame model has been created. The dimensions of the frame are shown in Fig. 6(a). The cross-sections of columns and beams in the frame are UC254×254×73 and UB UB356x171x51 respectively. It is assumed that a fire occurs in the right-hand bay of the lower storey, and that the beam and columns enclosing this bay are uniformly heated by fire. The temperatures of the left and right columns of the bay are 0.8 times the temperature of the beam. The uniformly distributed line loading applied to the beams is 26.8kN/m, giving them an ambient-temperature load ratio of 0.4 for fixed-ended conditions. The columns at ground floor level are loaded with a load ratio of 0.15. Flush end-plate connections are located at the ends of each beam. The connection dimensions are shown in Fig. 6(b). The stressed area of each bolt is set at 245mm<sup>2</sup>. Cases with and without the buckling element have been analysed. For cases with the buckling element, the buckling elements were located between the connection elements and their connected beam. In order to initiate beam-end flange buckling, full horizontal restraint has been applied at the frame edges.

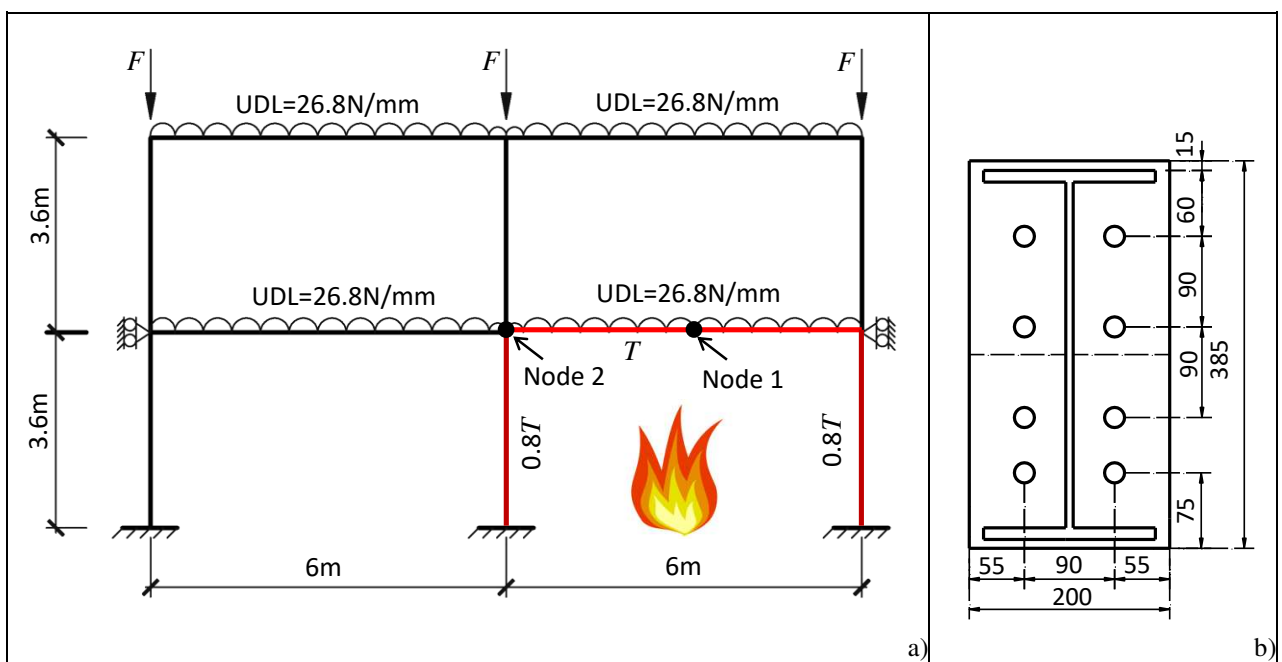


Fig. 6. Frame analysis: a) Studied frame dimension; b) Details of the connections

A comparison of vertical mid-span beam deflection (Node 1 in Fig. 6(a)) is shown in Fig. 7. It can be seen that, for the frame with the buckling element at beam-ends, the beam deflection increases due to the beam-end local buckling. Beam “run-away” caused by fracture of beam-end connections occurs later for frames containing the buckling elements.

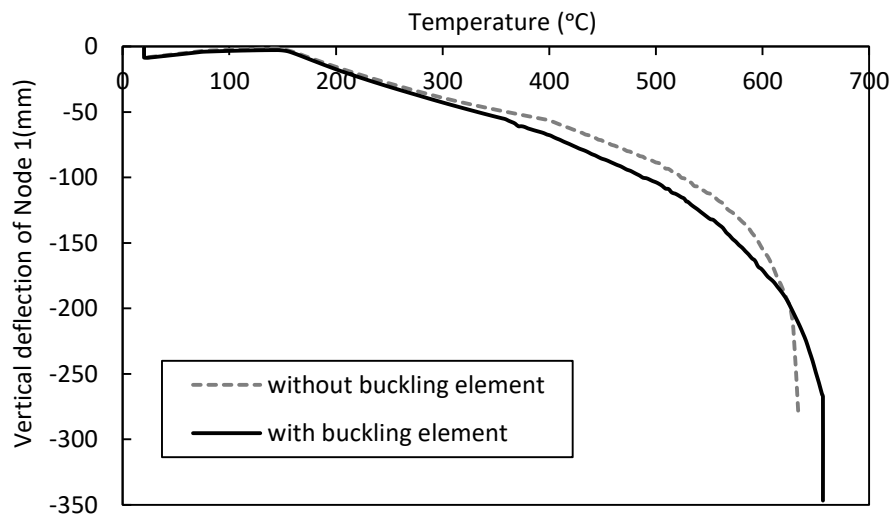
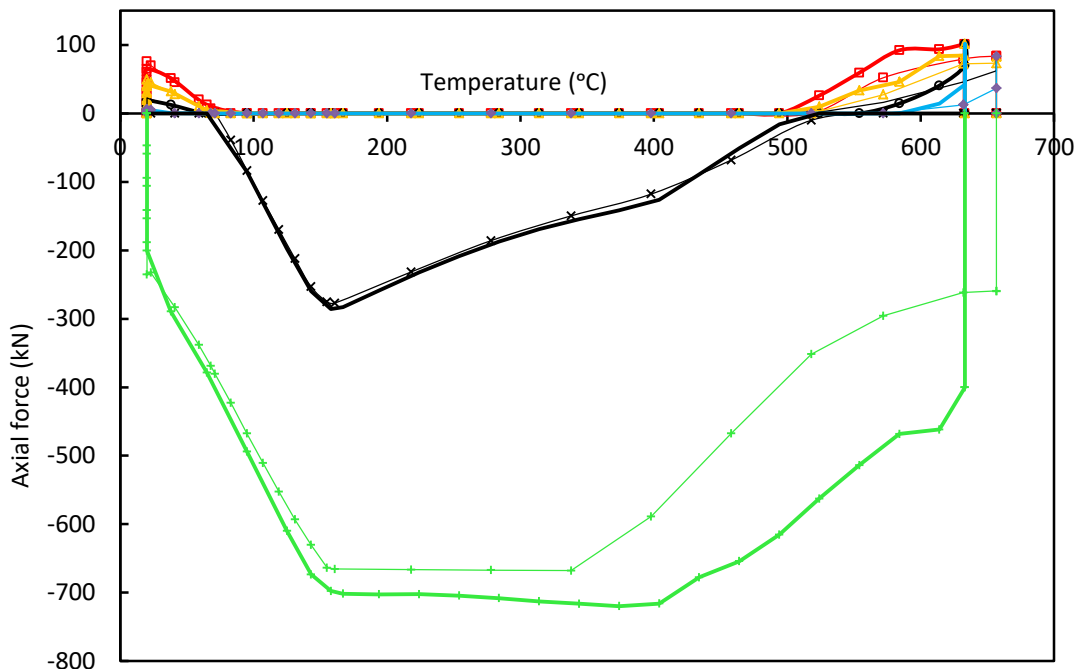


Fig. 7. Deflections of Node 1 for cases with and without the buckling element

Fig. 8 plots the axial forces of different components within the connection at the left hand side of the heated beam. Fig. 9 plots the detailed tension force within each bolt row. Comparisons of the axial component forces have been made for frames with and without buckling elements. It can be seen from Fig. 9 that each bolt row for the case with the adjacent buckling element fractures later than the bolt row at the same location for the case without the buckling element. The program run ends when all the connection bolt rows are fractured.



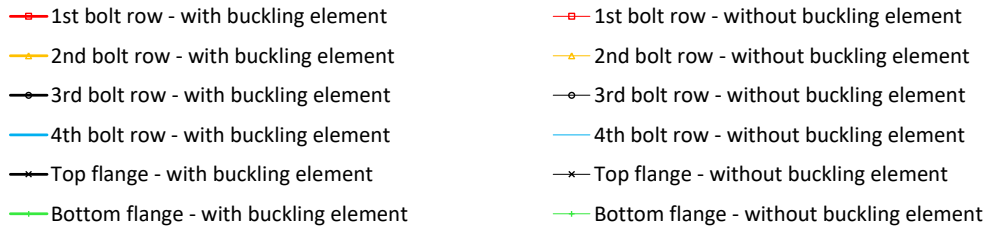


Fig. 8. Axial forces in different components of the analysed connection

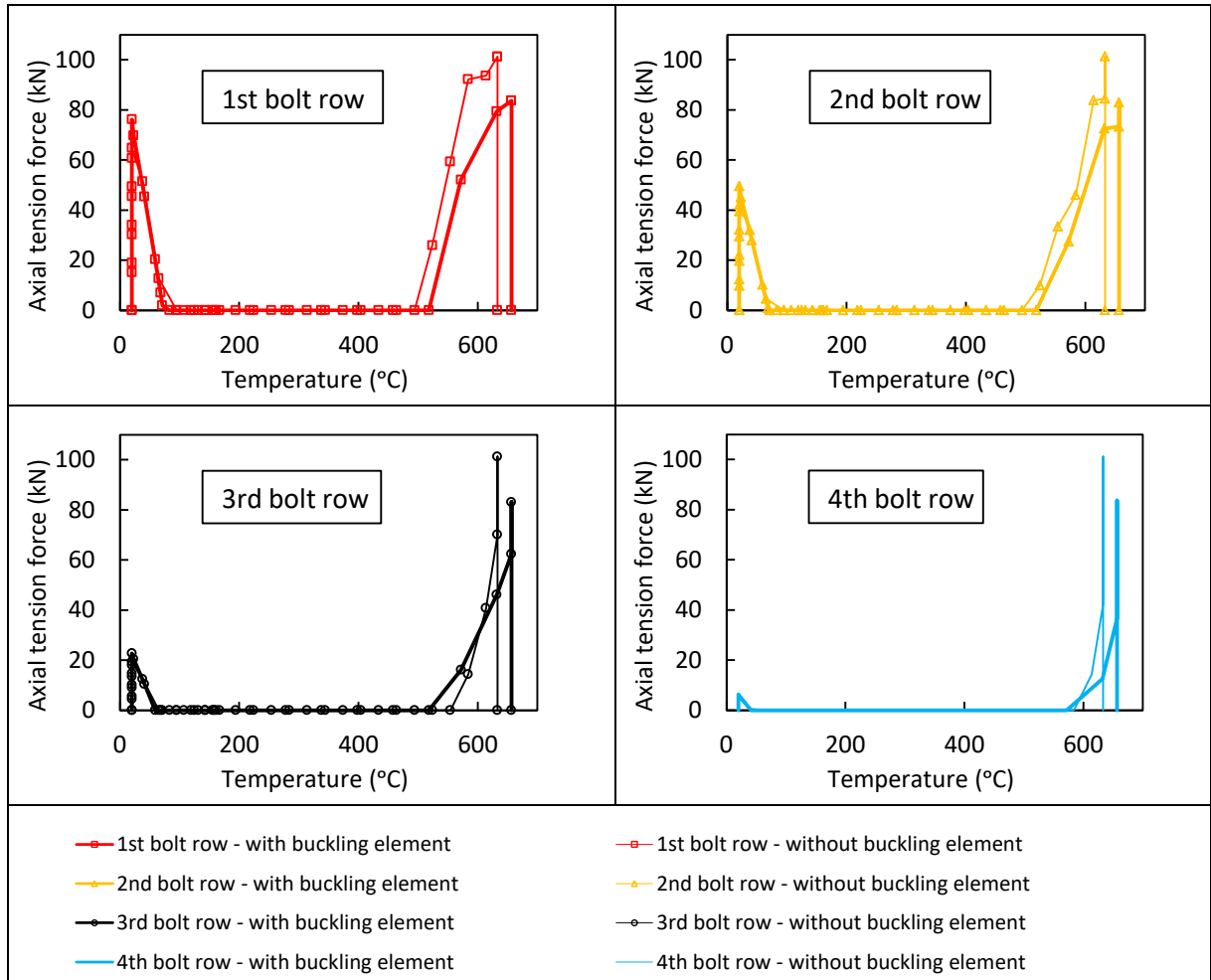


Fig. 9. Detailed bolt-row forces at Node 2

The vertical and horizontal displacements of Node 2 are shown in Fig. 10 and Fig. 11. It can be seen that this node has the same vertical displacements for cases with and without the buckling element. In the horizontal direction the latter case has smaller displacement compared with the former case, as shown in Fig. 11.

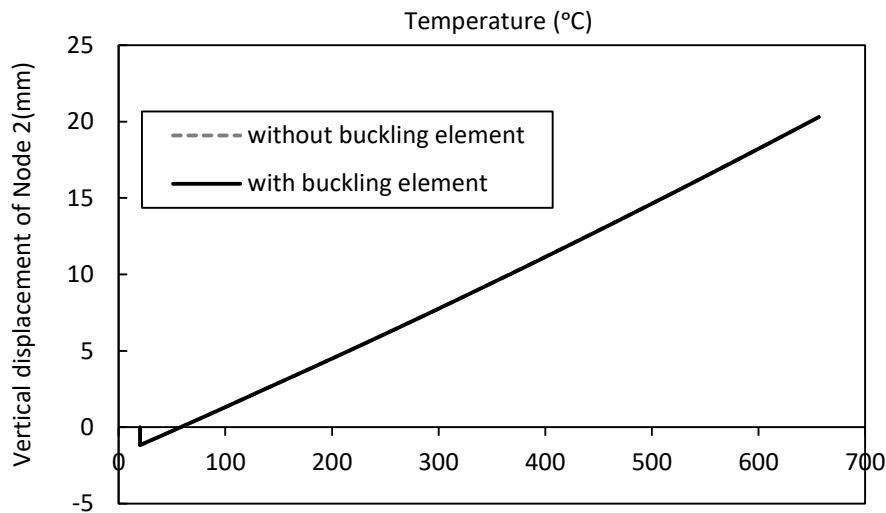


Fig. 10. Vertical displacement of Node 2

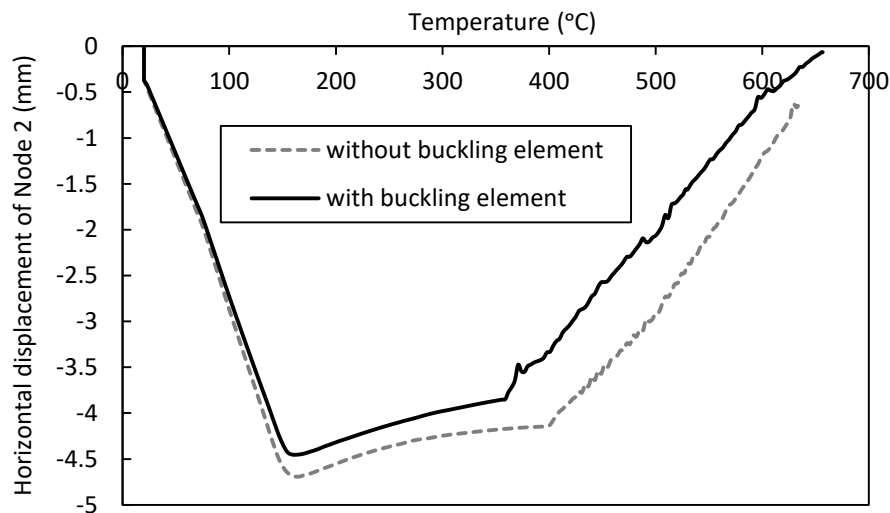


Fig. 11. Horizontal displacement of Node 2

#### 4 CONCLUSIONS

In this paper, the creation of a component-based model of the beam-end buckling zone has been described. The component-based model is able to represent the local beam-end buckling, including both bottom-flange buckling and beam-web shear buckling, at both ambient and elevated temperatures. The component-based model is composed of nonlinear springs. The flange springs are able to deal with the loading-unloading-reloading path. A significant challenge of this model is to deal with the descending post-buckling curve of the bottom-flange spring simultaneously with deformation reversal, because more than one solution can be found at a single force level in the solution process. On the post-buckling descending curve, an assumption of zero stiffness was made to overcome the double-solution problem. The component-based buckling element has been implemented in the 3D finite element software *Vulcan*. The influence of the buckling element on the adjacent connection has been investigated in a two-storey two-span plane frame. The results indicate that, by including the buckling element, both the net axial compression force and moment transferred from beam to connection have been reduced. The forces within the connection bolt rows are also reduced when the beam-end buckling is taken into consideration. Although the bolt forces adjacent to the buckling element are not reduced by a large amount, the trend is consistent in all the

cases analysed. Therefore, the existence of the buckling zones tends to protect the adjacent connections, as they decrease the connection bolt-row forces, and it is suggested that the modelling results tend to over-estimate the connection bolt row forces when the buckling phenomenon is ignored in practical design. Clearly, different types of connections need to be analysed to investigate the level to which this conclusion is true, or whether they are differently influenced by the occurrence of beam-end buckling.

## REFERENCES

- [1] Gann RG. “Final Report on the Collapse of World Trade Center Building 7, Federal Building and Fire Safety Investigation of the World Trade Center Disaster”, The National Institute of Standards and Technology (NIST), US, 2008
- [2] Newman G, Robinson JT and Bailey CG. “Fire safe design: A new approach to multi-storey steel-framed buildings”, Second Edition, The Steel Construction Institute, Berkshire, 2006
- [3] Spyrou S. “Development of a component based model of steel beam-to-column joints at elevated temperatures”, University of Sheffield: PhD thesis, 2002.
- [4] Block FM, Burgess IW, Davison JB, Plank RJ. “The development of a component-based connection element for endplate connections in fire”, *Fire Safety Journal* 42, pp.498-506, 2007
- [5] Al-Jabri KS, Davison JB, Burgess IW. “Performance of beam-to-column joints in fire—a review”, *Fire Safety Journal* 43, pp.50-62, 2008
- [6] Lennon T, Moore D. “Results and observations from full-scale fire test at BRE Cardington”, BRE client report, UK, 2004
- [7] Quan G, Huang S-S, Burgess I. “Component-based model of buckling panels of steel beams at elevated temperatures”, *Journal of Constructional Steel Research* 118, pp.91-104, 2016
- [8] Chiang, D.-Y. “The generalized Masing models for deteriorating hysteresis and cyclic plasticity”, *Applied Mathematical Modelling* 23, pp. 847-863, 1999